JOURNAL OF NANO- AND ELECTRONIC PHYSICS
Vol. 14 No 6, 06019(6pp) (2022)

ЖУРНАЛ НАНО- ТА ЕЛЕКТРОННОЇ ФІЗИКИ
Том 14 № 6, 06019(6cc) (2022)

Photoluminescence and Thermoluminescence Studies of Dysprosium (Dy^{3+}) Doped Zinc Aluminate Nanophosphor ($Zn_{0.97}Al_2O_4$:0.03Dy)

Pankaj Pathak[1,*], Manisha Singh[1,†], Pankaj Kumar Mishra[1], Ranjeet Brajpuriya[2]

[1] *Department of Applied Physics, Amity School of Pure and Applied Sciences, Amity University Madhya Pradesh, Maharajpura Dang, Gwalior, India*
[2] *Applied Science Cluster, University of Petroleum & Energy Studies, 248001 Dehradun, Uttrakhand, India*

(Received 26 October 2022; revised manuscript received 21 December 2022; published online 27 December 2022)

In the present paper, we have reported zinc aluminate ($ZnAl_2O_4$) doped with 0.03 mol. % of dysprosium (Dy^{3+}) nanophosphor with general formula $Zn_{(1-x)}Al_2O_4$:x(x = 0.03 mol. %)Dy for its luminescence properties and applications. Using urea as fuel, $ZnAl_2O_4$ doped with dysprosium (Dy^{3+}) nanophosphor was prepared by the combustion method. The synthesized nanophosphors were characterized with XRD, TEM, SEM with EDS and FTIR spectroscopy. From XRD studies, the average crystallite size was found to be 18.10 nm with space group $Fd^3{-}m$ and lattice parameters $a = b = c \sim 8.100$ Å. The selected area electron diffraction (SAED) revealed concentric circles which are due to polycrystallinity. The two peaks at 652.10 cm^{-1} and 545.19 cm^{-1} observed in FTIR spectroscopy correspond to aluminate (AlO6), which indicates the formation of $Zn_{0.97}Al_2O_4$:0.03Dy nanophosphor. For photoluminescence (PL) properties, a Xe lamp with 360 nm wavelength was utilized as an excitation source for the measurement. The excitation and emission spectra were evaluated in the range of 200 to 400 nm and 400 to 600 nm, respectively. An excitation peak at 305 nm was observed. For the excitation wavelength (λ_{ex} = 305 nm), emission spectra were recorded at 476 nm and 574 nm. For thermoluminescence (TL), the sample was pre-irradiated with high energy X-rays under Elekta Synergy radiation generating machine with a dose ranging from 500-1000 Gy. The kinetic parameters like activation energy and frequency factor were calculated from the TL glow curve. The results indicate that $Zn_{0.97}Al_2O_4$:0.03Dy could be a potential candidate as a blue-emitting diode and a high radiation passive dosimeter.

Keywords: Nanophosphors, Luminescence, Aluminates, XRD, FTIR, LED, Passive dosimeter.

DOI: 10.21272/jnep.14(6).06019 PACS numbers: 68.37.Hk,61.46.Hk, 61.05.cp, 78.60.Kn

1. INTRODUCTION

Due to high chemical stability and immense emission properties in the visible region, aluminate phosphors have extensively been studied [1-7]. $ZnAl_2O_4$ (ZA) is a semiconductor with an optical band gap (E_g) of 3.8-3.9 eV and can hold divalent and trivalent cations [8, 9], a representative material in the family of metal aluminates with a spinel structure, is widely used as a ceramic, electronic and catalytic material. Results have proved that aluminate-based nanophosphors are a promising host with high efficiency and stability. $ZnAl_2O_4$ nanophosphor doped with rare-earth metal ions is one of them with great potential. Rare-earth ions are widely used as activators in different hosts due to their high fluorescence efficiencies when the size of their particles is reduced to the nanoscale; these materials are widely used in diverse applications, such as in fluorescent lamps, cathode-ray tubes, light-emitting diodes (LEDs) for the lighting industry, field-emission displays and X-ray imaging [10-12]. Efforts have been devoted to studying the photoluminescence (PL) and thermoluminescence (TL) properties of Dy^{3+} doped $ZnAl_2O_4$ ($Zn_{0.97}Al_2O_4$:0.03Dy) and its applications in LEDs and passive dosimeters for high radiation TL dosimetry.

2. MATERIALS AND METHODS

Phosphors in the formula of $Zn_{0.97}Al_2O_4$:0.03Dy (x = 0.03 mol %) were prepared by the combustion synthesis method. The starting materials, magnesium nitrate [$Mg(NO_3)_3$] (99.99 %), aluminum nitrate [$Al(NO_3)_3$] (99.99 %) urea [NH_2-CO-NH_2] as fuel and dysprosium oxide [Dy_2O_3] (99.99 %), were mixed thoroughly in an agate mortar with the addition of a nitric acid. The mixtures were kept in an electrical muffle furnace for about 20 min at 550 °C. The general balanced chemical equations (1) and (2) represent the formation of $ZnAl_2O_4$ (pure) and $Zn_{0.97}Al_2O_4$:0.03Dy nanophosphors.

$$Zn_{(1-x)}(NO_3)_2 + 2Al(NO_3)_3 + 6.67NH_2 - CO - NH_2 + X(x=0)Dy = ZnAl_2O_4 + 6.67CO_2 + 13.33H_2O + 10.67N_2 \quad (1)$$

$$Zn(NO_3)_2 + 2Al(NO_3)_3 + 7.166NH_2 - CO - NH_2 + X(x=0.03\ mol\ \%)Dy_2O_3 = Zn_{0.97}Al_2O_4:0.03Dy + 7.166CO_2 + 14.33H_2O\ 11.167N_2 \quad (2)$$

The synthesized sample was investigated on a Rigaku's Miniflex 600 Benchtop X-ray diffraction (XRD) instrument at Dr APJ Abdul Kalam Central Instrumentation Facility (CIF), Jiwaji University, Gwalior (MP) with CuKα [40 kV, 15 mA X-ray] at λ = 1.54 Å. The mean crystallite size of the powder was calculated by employing the Debye-Scherrer formula and the interplanar spacing (d) and lattice parameters were calculated by the Bragg's law.

* pankaj2002@hotmail.com
† msingh@gwa.amity.edu

The crystal structure and the difference in microstructure between the materials were further studied by TEM. For validation of XRD, pure $ZnAl_2O_4$ was selected for TEM and SAED analysis. A pure $ZnAl_2O_4$ sample was selected to confirm the fact that the crystal structure hardly changes after adding a small amount of dopants.

Further, a JEOL JSM-6390LV scanning electron microscope (with EDS) was employed to investigate the morphological properties and elemental contents of each material present in the synthesized nanophosphor. Fourier transform infrared (PerkinElmer Spectrum Version10.4.00) spectroscopy was used to determine the different stretching mode frequencies, functional and fingerprint groups present in the samples.

3. RESULTS AND DISCUSSION

The XRD pattern of $Zn_{0.97}Al_2O_4$:0.03Dy nanophosphor is illustrated in Fig. 1. The position and intensity of the diffraction peaks are well-matched to the (220), (311), (400), (422), (511), (440), (620), (533) planes of the prepared $Zn_{0.97}Al_2O_4$:0.03Dy with the Joint Committee Powder Diffraction Standard file (JCPDS: 82-1539). The reference XRD pattern of zinc aluminate ($ZnAl_2O_4$) is also shown for comparison in Fig. 1. The Debye-Scherrer equation was used to determine the particle size from the full width at half maximum (FWHM) of the characteristics peak [13, 14]. According to calculations made using data from the XRD (311) plane and the width of the peak at $2\theta \sim 36.69$, the average crystallite size of $Zn_{0.97}Al_2O_4$:0.03Dy nanophosphor was found to be 18.10 nm. Table 1 shows the locations of the XRD pattern (311) peak as well as the calculated lattice parameters (a, b, and c) based on the Bragg law and the distance between crystal planes (d-spacing). The crystal structure of synthesized $Zn_{0.97}Al_2O_4$:0.03Dy nanophosphor belongs to the cubic close-packed structure with space group Fd^3-m with lattice parameters $a = b = c \sim 8.09$ Å which precisely matches the standard lattice parameters ~ 8.0875 Å. This evidences that the formed nanostructure exhibits spinel structure.

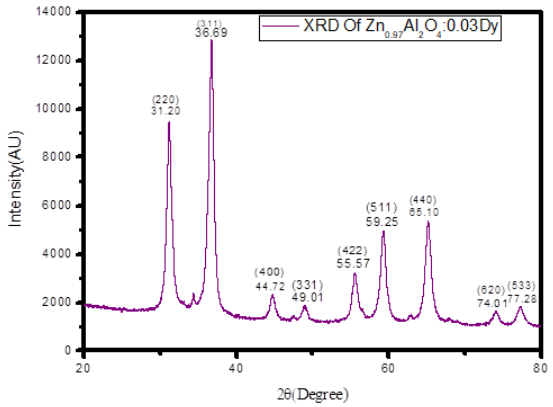

Fig. 1 – XRD pattern of $Zn_{0.97}Al_2O_4$:0.03Dy nanophosphor

Table 1 – Position of the peak (311) of XRD patterns and the calculated values of the crystal planes spacing and lattice parameters

Nanophosphor	2θ (degree)	d-spacing (Å)	Lattice parameters ($a = b = c$) (Å)
$Zn_{0.97}Al_2O_4$:0.03Dy	36.69	2.44	8.09

Fig. 2 shows TEM images of pure $ZnAl_2O_4$.

The selected area electron diffraction (SAED) patterns are used to determine the d spacing of the crystal planes in a single or polycrystalline structure. The SAED patterns of pure $ZnAl_2O_4$ in Fig. 3 show concentric circles which are due to polycrystallinity of the nanostructure. Table 2 represents the d-spacing and (hkl) planes of pure $ZnAl_2O_4$ calculated from the main diffraction rings using ImageJ software, where $2r$ is the diameter of the rings, and r is the radius of the rings which represents the d-spacing of the crystalline plane of pure $ZnAl_2O_4$. The (hkl) values are then computed from standard JCPDS Card 82-1539 for pure $ZnAl_2O_4$.

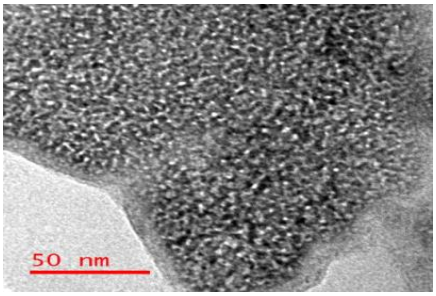

Fig. 2 – TEM images of pure $ZnAl_2O_4$

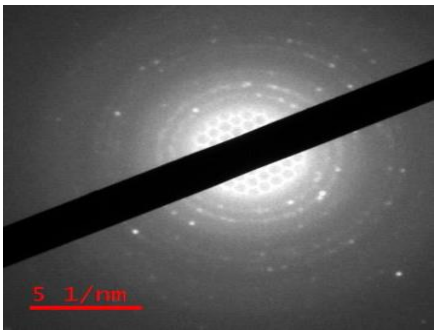

Fig. 3 – SAED pattern of pure $ZnAl_2O_4$

Table 2 – Determination of the d-spacing and associated (hkl) from main diffraction rings of SAED pattern of pure $ZnAl_2O_4$

S. No.	$1/2r$ (nm^{-1})	$1/r$ (nm^{-1})	r (nm^{-1})	d-spacing (Å)	(hkl)
1	6.857	3.4285	0.29167	2.91	220
2	8.408	4.204	0.23787	2.37	311
3	9.582	4.791	0.20873	2.08	400
4	12.196	6.098	0.16399	1.63	422
5	13.674	6.837	0.14626	1.46	440
6	15.872	7.936	0.12601	1.26	533

The primary diffraction rings are connected to the (220), (311), (400), (422), (440), and (533) planes of pure $ZnAl_2O_4$ nanophosphor. In the SAED patterns, we discovered the (220), (311), (400), (422), (440), and (533) planes, which are also present in the XRD of pure $ZnAl_2O_4$. This indicates a strong correlation between TEM and XRD study results.

The SEM image with a different magnification of $Zn_{0.97}Al_2O_4$:0.03Dy is shown in Fig. 4. The surface morphology of the particles was not uniform, and it can be observed from the SEM image that the prepared sample consists of particles with different size distribution.

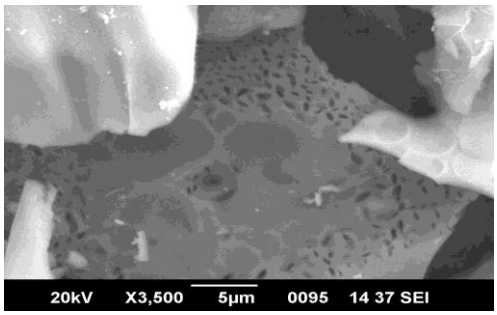

Fig. 4 – SEM images of $Zn_{0.97}Al_2O_4$:0.03Dy

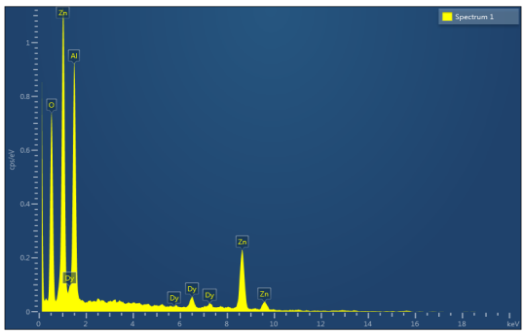

Fig. 5 – EDX spectrum 1 of $Zn_{0.97}Al_2O_4$:0.03Dy

Energy dispersive X-ray spectroscopy (EDX) is a very useful tool for identifying homogeneity and the elemental content of each material present in the synthesized nanophosphor. To confirm the formation of $Zn_{0.97}Al_2O_4$:0.03Dy, complex EDX analysis was performed at DST-SAIF Kochi, Kerala (India). Different areas were concentrated during the EDX measurement, and the corresponding peaks are shown in Fig. 5. The EDS/EDX results in weight % and atomic % of $Zn_{0.97}Al_2O_4$:0.03Dy, the quantities of oxygen (O), magnesium (Mg), aluminum (Al), zinc (Zn), dysprosium (Dy) were 57.16, 15.14, 26.48, 1.22, respectively, as shown in Fig. 5.

Details of the EDX spectra of $Zn_{0.97}Al_2O_4$:0.03Dy nanophosphor with values measured in weight and atomic % are listed in Table 3.

An FTIR spectroscopy tool was used to further investigate the appearance of the phases and the purity of the results. The middle infrared (IR) region (from 4000 to 400 cm^{-1}) of the FTIR spectra of the synthesized $Zn_{0.97}Al_2O_4$:0.03Dy is shown in Fig. 6.

$Zn_{0.97}Al_2O_4$:0.03Dy (UATR, vma × cm^{-1}): 3026.21 (v=C–H, Stretch, Aromatics), 1743.22 (v=C=O, Stretch, Aldehyde saturated aliphatics), 1371.23 (v=N–O, Asymmetric, Stretch, Nitro Compound), 1218.37 (v=C–N, Stretch, Aliphatic).

Table 3 – Elemental composition of $Zn_{0.97}Al_2O_4$:0.03Dy nanophosphor with weight (wt.) and atomic % in the EDX spectra

$Zn_{0.97}Al_2O_4$:0.03Dy	Spectrum 1	
Elements	wt. %	atomic %
O(K)	32.47	57.16
Zn(K)	25.37	15.14
Al(K)	35.14	26.48
Dy(L)	7.03	1.22
Total	100	100

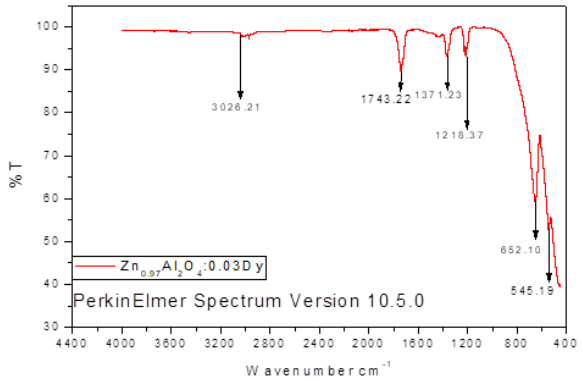

Fig. 6 – FTIR of $Zn_{0.97}Al_2O_4$:0.03Dy

However, vibrations at 3026.21-2852.93 cm^{-1} for $Zn_{0.97}Al_2O_4$:0.03Dy appeared within the IR spectra due to CH stretching and aromatics functional group. The peak at 1748.82-1743.22 cm^{-1} for $Zn_{0.97}Al_2O_4$:0.03Dy is due to C=O stretching and aldehyde saturated aliphatic functional group. This might be the absorption of CO_2 and moisture from the air [16]. The peak at 1384.74-1371.23 cm^{-1} for $Zn_{0.97}Al_2O_4$:0.03Dy is due to N–O asymmetric stretching nitro compounds formed due to the presence of nitrates [$Mg(NO_3)_2$, $Al(NO_3)_3$, and $Zn(NO_3)_2$ raw materials [15]]. The small peak at around 1229.78-1218.37 cm^{-1} for $Zn_{0.97}Al_2O_4$:0.03Dy is observed due to C–N stretching and aliphatic group.

3.1 Thermoluminescence (TL) Analysis of $Zn_{0.97}Al_2O_4$:0.03Dy

A thermoluminescence reader (Integral-Pc Based) Nucleonix TL 1009I (Source: Pt. Ravishankar Shukla University, CG-India) was utilized in this work for TL analysis. The creation of materials for high-radiation TL dosimetry has received particular focus. Numerous researchers who have standardized a variety of materials for TL dosimetry have found that luminescent material can be used in radiation dose estimation in TLD if it meets certain minimum requirements (dosimetric properties) [17]. In our work, the amount of pre-irradiated powdered nanophosphors was kept constant (8 mg) each time in the TL reader for the TL measurement. The heating rate in our study during the measurement was 5 °C/s.

3.1.1 TL Glow Curve

The TL glow curve was fitted by using Gaussian curve fitting. The single peaks were observed in the synthesized nanophosphors that may be due to intrinsic defects, and to find the effects of irradiation doses and concentration of Dy^{3+}, the relative intensity of each peak of synthesized nanophosphors was calculated. The TL glow curve of $Zn_{0.97}Al_2O_4$:0.03Dy for doses ranging in 500-1000Gy nanophosphors is shown in Fig. 7.

The peak temperature (T_m) from the TL glow curve was found equal to 216 °C, 228 °C, 215 °C and 224 °C for $Zn_{0.97}Al_2O_4$:0.03Dy at doses of 500-1000Gy. Small temperature changes in the glow peaks (± 10 degrees) are caused by long-range lattice distortions, which are sensitive to impurities and their concentration [18]. The fact that the peak temperature position changed as

the radiation dose value changed suggests that the TL peak under study does not exhibit first-order kinetic behavior [19]. Table 4 and Table 5 show the peak temperature and relative TL intensity from the TL glow curve of $Zn_{0.97}Al_2O_4$:0.03Dy nanophosphor at doses of 500-1000 Gy.

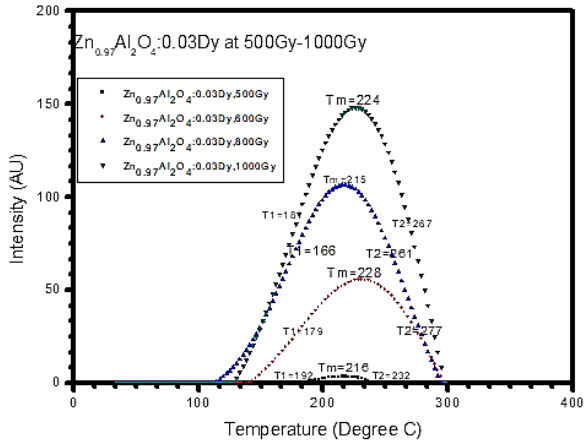

Fig. 7 – TL glow curve of $Zn_{0.97}Al_2O_4$:0.03Dy at doses 500-1000 Gy

It has been noticed from the relative TL intensity that the synthesized nanophosphor shows a continuous increase in TL intensity with an increase in dose and maximum at a dose of 1000 Gy. The reason for this is assumed that on increasing dose, trapped electrons are released and recombine with holes, causing luminescence. But the response of dose on TL intensity was still unanswered. For this, the TL dose-response curve was plotted and analyzed.

Table 4 – Peak temperatures from the TL glow curve of $Zn_{0.97}Al_2O_4$:0.03Dy nanophosphor

Phosphor	T_m, °C (500 Gy)	T_m, °C (600 Gy)	T_m, °C (800 Gy)	T_m, °C (1000 Gy)
$Zn_{0.97}Al_2O_4$: 0.03Dy	216	228	215	224

Table 5 – Relative TL intensity from the TL glow curve of $Zn_{0.97}Al_2O_4$:0.03Dy nanophosphor

Phosphor	Relative TL intensity (500Gy)	Relative TL intensity (600Gy)	Relative TL intensity (800Gy)	Relative TL intensity (1000Gy)
$Zn_{0.97}Al_2O_4$: 0.03Dy	0.02	0.37	0.70	1.00

3.1.2 TL Dose-Response Curve

To estimate a radiation dose using the TL technique, it is important to record the TL response of the sample under study at various radiation doses. To use the dosimetric characteristic of the material under study, TL intensity should increase linearly with the lengthening of radiation exposure for it. Fading is strongly dependent on peak temperature [18].

Fig. 8 shows the TL dose-response curve of $Zn_{0.97}Al_2O_4$:0.03Dy nanophosphor. It is noted that the intensity rises nearly linearly for all doses between 500 to 1000 Gy.

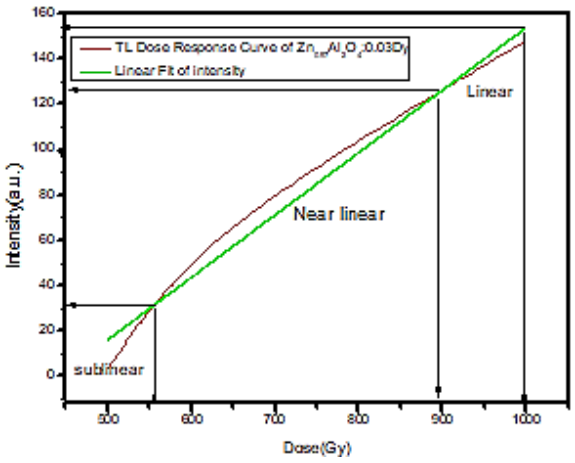

Fig. 8 – TL dose response curve for $Zn_{0.97}Al_2O_4$:0.03Dy

3.1.3 Determination and Analysis of Kinetic Parameters for $Zn_{0.97}Al_2O_4$:0.03Dy

Equations (3) and (4) were used to calculate the kinetic parameters such as activation energy, frequency factor, shape factor, and their dependent parameters, as well as the total half-width intensity (ω), half-width at the low-temperature side of the peak (τ) and half-width towards the fall-off side of the glow peak (δ):

$$E = 2KTm[1.76 \cdot (Tm \ / \omega) - 1], \quad (3)$$

where E is the activation energy in eV, K is the Boltzmann constant ($eV \cdot K^{-1}$), ω is the total half-width intensity ($\omega = \tau + \delta$), τ is the half-width at the low-temperature side of the peak ($\tau = T_m - T_1$), δ is the half-width towards the fall-off side of the glow peak ($\delta = T_2 - T_m$), and T_m is the peak temperature at the maximum TL intensity.

In order to distinguish the first- and second-order TL glow peaks, the geometrical factor ($\mu g = \delta/\omega$) is used. First-order kinetics $\mu g = 0.39$-0.42; second-order kinetics $\mu g = 0.49$-0.52; and mixed-order kinetics $\mu g = 0.43$-0.48 [20]. The activation energy E and the frequency factor s are related by the equation (3):

$$\beta E / KT_m^{\,2} = s\left[1 + (b-1) \times 2KT_m / E\right] Exp\left(E / KT_m\right), \quad (4)$$

where b is the order of kinetics and β is the heating rate equal to $5^{o}Cs^{-1}$ for our work.

The effect of X-ray irradiation (doses ranging from 500-1000 Gy) on TL parameters of the synthesized nanophosphor is illustrated in Table 6. The shape factor (μg) lies between 0.40-0.51 for $Zn_{0.97}Al_2O_4$:0.03Dy which reveals that this nanophosphor approaches the second order kinetics [20]. The activation energy (E) or depth of trap levels ranges from 0.67 to 1.72 eV as illustrated in Table 6.

Kinetic Parameters of $Zn_{0.97}Al_2O_4$:0.03Dy. It has been noticed that the activation energy and frequency order increase at 500 Gy and decrease at 600 Gy and 800 Gy and again increase at 1000 Gy overall, shifting the peaks towards higher temperatures and wider peaks. Also, it has been observed that the TL intensity increases with increasing doses and is maximum for 1000 Gy.

Table 6 – TL parameters for the glow peaks of synthesized $Zn_{0.97}Al_2O_4$:0.03Dy

Dose (Gy)	500	600	800	1000
HTR (°C/S)	5	5	5	5
T_1, °C	192	179	166	184
T_m, °C	216	228	215	224
T_2, °C	232	277	261	267
τ°C	24	49	49	40
δ	16	49	46	43
ω	40	98	95	83
μ	0.4	0.5	0.48	0.51
Activation energy(E) (eV)	1.72	0.69	0.67	0.81
Frequency factor (S^{-1})	14.00×10^{11}	6.29×10^{11}	5.84×10^{11}	7.19×10^{11}

3.2 Photoluminescence (PL) Analysis of $Zn_{0.97}Al_2O_4$:0.03Dy

PL studies were carried out for $Zn_{0.97}Al_2O_4$:0.03Dy abbreviated as R1 nanophosphor to investigate the application of the synthesized nanophosphors for long afterglow and color displays. It is used specially to achieve the details about defects of nanophosphors. The light is applied through the sample which stimulates the defects from lower level to higher level. Coming back to the original (lower) level causes the emission of a photon. It was observed that the synthesized phosphors satisfy the essential requirements of an ideal long afterglow and color displays.

To study the PL properties of the prepared $Zn_{0.97}Al_2O_4$:0.03Dy (R_1) nanophosphor, a Xe lamp with 360 nm wavelength was utilized as an excitation source for the measurement. The excitation and emission spectra were evaluated in the range from 200 to 400 nm and 400 to 600 nm, respectively. From Fig. 9 in the excitation spectra of $Zn_{0.97}Al_2O_4$:0.03Dy (R_1), an excitation spectrum (peak) is observed at 305 nm. For the excitation wavelength ($\lambda_{ex} = 305$ nm), emission spectra (peak) were recorded at 476 nm and 574 nm, as illustrated in Fig. 10. The blue (476 nm) and yellow (574 nm) emission spectra are typical emissions of Dy^{3+} corresponding to the $_4F^{9/2} - {}_6H^{15/2}$, $_6H^{13/2}$ transitions, respectively [21].

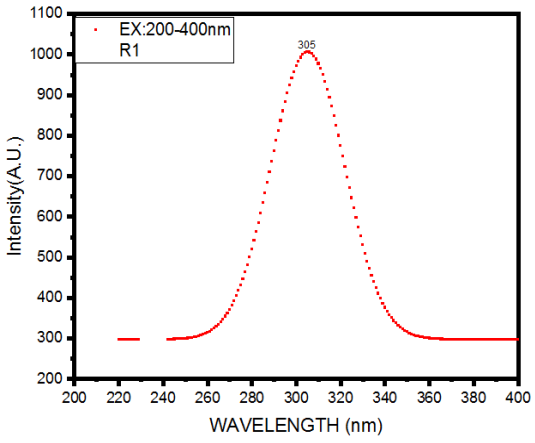

Fig. 9 – Excitation spectra of $Zn_{0.97}Al_2O_4$:0.03Dy (R_1) nanophosphor

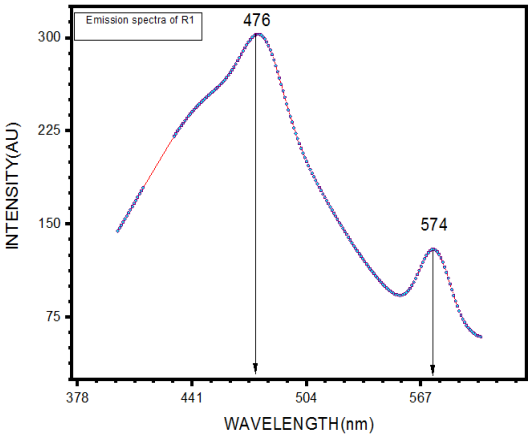

Fig. 10 – Emission spectra of $Zn_{0.97}Al_2O_4$:0.03Dy (R_1) nanophosphor

3.2.1 Chromaticity Diagram of $Zn_{0.97}Al_2O_4$:0.03Dy (R_1)

Further the study was extended to investigate the color of the synthesized luminescent crystal by employing color coordinates. By using the PL data and the interactive software (CIE coordinate calculator), the emission spectra (peak) of the $Zn_{0.97}Al_2O_4$:0.03Dy (R_1) nanophosphor were transformed into the CIE 1931 chromaticity diagram, as illustrated in Fig. 11. This is represented as the point 'o' with the CIE coordinate [x, y]. Fig. 11 illustrates the CIE 1931 diagram and the chromaticity values for $Zn_{0.97}Al_2O_4$:0.03Dy phosphor. The values of X and Y coordinates of the system were calculated to be [$X = 0.19$, $Y = 0.24$], respectively, which is following the chromaticity values of reference blue light. It is understood from the values that, $Zn_{0.97}Al_2O_4$:0.03Dy (R_1) phosphor, as illustrated in Fig. 11, gives blue light emission.

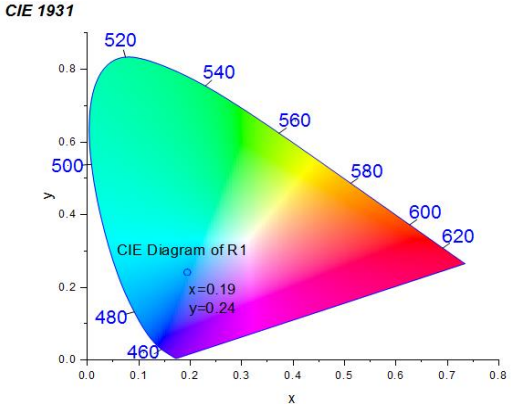

Fig. 11 – CIE chromaticity diagram of $Zn_{0.97}Al_2O_4$:0.03Dy (R_1) phosphor

4. CONCLUSIONS

According to XRD analysis, the synthesized nanophosphor has spinel-type structures, which are typically cubic close-packed oxides with 8 tetrahedral and 4 octahedral sites per formula unit, and space group $Fd^{-3}m$. The average crystallite size of nanophosphor was found to be in the range of 45.36 nm. From SEM, the sample exhibits cylindrical shapes. The EDX spectra of the synthesized nanophosphor showed the pres-

ence of all constituent elements of the sample. FTIR spectra of the synthesized nanophosphor showed the peaks and absorption bands of aluminates groups, thereby confirming the aluminate group in the sample. Less fading and high stability of the synthesized sample are shown by the peak temperatures (T_m) from the TL glow curve of $Zn_{0.97}Al_2O_4$:0.03Dy that were discovered at high temperatures. Here, deep trapping in the sample was developed as indicated by high-temperature peaks. It was found from the dose-response curve of the $Zn_{0.97}Al_2O_4$:0.03Dy sample that intensity increases linearly with an increase in dose, making it a prospective candidate for high-dose radiation TL dosimetry. The kinetic parameters such as activation energies and frequency factors showed deep traps and high activation energies, making them ideal for applications in passive dosimeters for high radiation TL dosimetry. For an excitation wavelength of 305 nm, emission spectra (peaks) at 476 nm and 574 nm were observed for $Zn_{0.97}Al_2O_4$:0.03Dy. Emission at 476 nm is more prominent than emission at 574 nm. This transition confirms that Dy^{3+} not only creates deep traps, but also acts as a luminescence center. Hence, these nanophosphors can be used for long blue afterglow displays.

REFERENCES

1. K. Yokota, S.X. Zhang, K. Kimura, *J. Lumin.* **92**, 223 (2001).
2. D. Ravichandran, R. Roy, W.B. White, S. Erdei, *J. Mater. Res.* **12**, 819 (1997).
3. A. Ellens, F. Zwaschka, F. Kummer, A. Meijerink, M. Raukas, K. Mishra, *J. Lumin.* **93**, 147 (2001).
4. D. Jia, R.S. Meltzer, W.M. Yen, W. Jia, X.J. Wang, *Appl. Phys. Lett.* **80**, 1535 (2002).
5. Z. Fu, S. Zhong, S. Zhang, *J. Phys. Chem. B* **109**, 14396 (2005).
6. Z. Xu, Y. Li, Z. Liu, D. Wang, *J. Alloy. Compd.* **391**, 202 (2005).
7. H. Nakagawa, K. Ebisu, M. Zhang, M. Kitaura, *J. Lumin.* **102**, 590 (2003).
8. C. Pratapkumar, S.C. Prashantha, H. Nagabhushana Pratapkuma, D.M. Jnaneshwara, *J. Sci.: Adv. Mater. Dev.* **3**, 464 (2018).
9. P. Kumari, Y. Dwivedi, *J. Lumin.* **178**, 407 (2016).
10. J.A. de Pooter, A.B. Bril, *J. Elctrochem. Soc.* **122**, 1086 (1975).
11. A. Fernández-Osorio, C.E. Rivera, J. Chávez; *Proceedings of the World Congress on New Technologies (NewTech 2015) Barcelona, Spain* (2015) Paper No. 360.
12. I. Miron, C. Enache, I. Grozescu, *Digest J. Nanomat. Biostruct.* **7**, 967 (2012).
13. P.Vasilis, K. George, F. Claudio Furetta, *Numerical and Practical Exercises in Thermoluminescence* (New York, NY: Springer New York: 2006).
14. Singanahally T. Aruna, Alexander S. Mukasyan, *Curr. Opin. Solid State Mater. Sci.* **12**, 44 (2008).
15. T. Viswanathan, S. Pal, A. Rahaman, *Sādhanā* **45**, 17 (2020).
16. S. Tripathy, D. Bhattacharya, *J. Asian Ceram. Soc.* **1**, 328 (2013).
17. K. Lemański, et al., *J. Rare Earths* **32** No 3 265 (2014).
18. V. Dubey, V.P. Dubey, R.K. Tamrakar, K. Upadhyay, N. Tiwari, *J. Radiation Res. Appl. Sci.* **8** No 1, 126 (2015).
19. A. Ege, Y. Wang, P.D. Townsend, *Nucl. Instrum. Meth. Phys. Res., Section A* **576** No 2-3, 411 (2007).
20. V. Pagonis, G. Kitis, C. Furetta, *Numerical and Practical Exercises in Thermoluminescence* (New York, NY: Springer New York: 2006).
21. S.F. Wang et al., *J. Alloy. Compd.* **394** No 1-2, 255 (2005).

Дослідження фотолюмінесценції та термолюмінесценції нанолюмінофору алюмінату цинку, легованого диспрозієм (Dy^{3+}) ($Zn_{0.97}Al_2O_4$:0.03Dy)

Pankaj Pathak[1], Manisha Singh[1], Pankaj Kumar Mishra[1], Ranjeet Brajpuriya[2]

[1] *Department of Applied Physics, Amity School of Pure and Applied Sciences, Amity University Madhya Pradesh, Maharajpura Dang, Gwalior, India*

[2] *Applied Science Cluster, University of Petroleum & Energy Studies, 248001 Dehradun, Uttrakhand, India*

У статті ми повідомляємо про алюмінат цинку ($ZnAl_2O_4$), легований нанолюмінофором з 0,03 моль % диспрозію (Dy^{3+}), із загальною формулою $Zn_{(1-x)}Al_2O_4$:x(x = 0.03 mol. %)Dy завдяки його люмінесцентним властивостям та різним застосування. З використанням сечовини як палива методом спалювання отримано нанолюмінофор $ZnAl_2O_4$, легований диспрозієм (Dy^{3+}). Синтезовані нанолюмінофори були охарактеризовані за допомогою XRD, TEM, SEM з EDS та FTIR спектроскопією. За результатами XRD досліджень було встановлено, що середній розмір кристалітів становить 18,10 нм з просторовою групою $Fd\bar{3}m$ і параметрами решітки $a = b = c \sim 8.100$ Å. Електронна дифракція вибраної області (SAED) виявила концентричні кола, зумовлені полікристалічністю. Два піки при 652,10 $см^{-1}$ і 545,19 $см^{-1}$, які спостерігаються за допомогою FTIR спектроскопії, відповідають алюмінату (AlO_6), що вказує на утворення нанолюмінофора $Zn_{0.97}Al_2O_4$:0.03Dy. Для дослідження фотолюмінісцентних (PL) властивостей використовувалася лампа Xe з довжиною хвилі 360 нм як джерело збудження. Спектри збудження та випромінювання оцінювали в діапазоні від 200 до 400 нм та від 400 до 600 нм відповідно. Пік збудження спостерігався при 305 нм. Для довжини хвилі збудження (λ_{ex} = 305 нм) спектри випромінювання записували при 476 нм і 574 нм. Для дослідження термолюмінесценції (TL) зразок був попередньо опромінений рентгенівським випромінюванням високої енергії з дозою в діапазоні від 500 до 1000 Gy. Кінетичні параметри, такі як енергія активації та частотний фактор, були розраховані за кривою світіння TL. Результати показують, що $Zn_{0.97}Al_2O_4$:0.03Dy може бути потенційно використаний як синій випромінюючий діод та пасивний дозиметр з високою радіацією.

Ключові слова: Нанолюмінофори, Люмінесценція, Алюмінати, XRD, FTIR, LED, Пасивний дозиметр.